Transcriptomic and metabolomic analyses of the response of sainfoin (Onobrychis viciifolia) seedings to low-temperature stress

Jiao Cheng
Gansu Agricultural University
kun Wang
Gansu Agricultural University
Yuheng Yao
Gansu Agricultural University
Shiwen Wu
Gansu Agricultural University
Lili Nan
nanll@gsau.edu.cn

Gansu Agricultural University

Research Article

Keywords: sainfoin, transcriptome, metabolome, anthocyanins biosynthesis, amino acid metabolism, metabolic network

Posted Date: April 22nd, 2024

DOI: https://doi.org/10.21203/rs.3.rs-4241762/v1

Additional Declarations: No competing interests reported.

Abstract

Sainfoin (*Onobrychis viciifolia*) is a valuable native legume forage in northwest China and is commonly used as fodder for livestock. However, low temperatures (LW) not only affect the yield and quality of sainfoin but also its geographical distribution. The leaves of the cold-tolerant new line of P4 and the cold-sensitive material of 13709 were collected after low temperature (4℃) treatment to evaluate their molecular regulatory mechanisms during low temperature via integrative analyses of their transcriptomes and metabolomes. A comprehensive analysis was conducted, including the detection of 6619 metabolites and annotation of 6939 genes using UPLC-MS/MS analysis and the IIIumina HisSeq system. The metabolomics analysis revealed 26 common differentially accumulated metabolites (DAMs) in the cold-tolerant and cold-sensitive sainfoin at different comparisons, these metabolites are mainly divided into lipids and lipid-like molecules, and phenylpropanoids and polyketides. Transcriptome analysis identified 1045, 1412, 5010, and 3119 differentially expressed genes (DEGs) in different comparisons at the same time points. By integrating the transcriptomic and metabolomic datasets, it was observed that several DAMs were closely associated with DEGs. Functional enrichment analysis of DAMs and associated DEGs highlighted their involvement in anthocyanin biosynthesis and amino acid metabolism. Six candidate genes from the above pathways were selected for controlling the adaptation to LW stress. These findings provide valuable insights into the metabolic regulation of sainfoin under LW stress and offer guidance for improving its cold resistance and selecting cold-tolerant varieties.

1 Introduction

Sainfoin (*Onobrychis viciifolia*) is a native forage in the northwest region of China, widely distributed in temperate regions such as Gansu, Inner Mongolia, Qinghai, and other areas [1]. Often dubbed ‘the queen of forages’, it boasts numerous superior traits, including high yield, excellent herbage quality, soil improvement, biological nitrogen fixation, and ecological protection [2]. As a consequence, it finds extensive use in animal husbandry and ecological restoration in China. Nevertheless, the colder winter temperatures and severe spring inversions in the northern pastoral areas of China can lead to frost damage to crops, and in severe cases, even plant mortality [3]. Although sainfoin can adapt to environmental stress, LW stress is an essential factor that affects its geographical distribution [4]. Investigations on LW stress responses and regulatory pathways are important for breeding new sainfoin cultivars with preeminent cold-resistant varieties.

To perceive and adapt to adverse LW stress conditions, plants have evolved effective regulatory mechanisms to improve cold tolerance [5]. Cold-induced gene (COR) is a kind of gene regulated by cold stress, which can be activated under the stimulation of low temperatures and short days to produce cold regulatory protein and improve the cold resistance of plants [6]. The study found that the *cis*-acting element (CRT) of the dehydration response element (DRE) is related to LW stress in the promoter region of the COR gene, and some COR genes are activated by C-cyclic peptide binding transcription factor (CBF), that is, through the ICE-CBF-COR signaling pathway [5]. CBF (C-repeat binding transcription factor/dehydrate responsive element binding factor, DREB) specifically binds to the CRT/DRF *cis*-acting

element in the promoter region to activate the cold resistance response [6]. So far, the ICE-CBF-COR pathway is recognized to play a central role in the regulation of cold stress response [7]. In addition to the CBF cold stress response pathway, other genes also play an important role in the regulation of cold stress response. For instance, the R2R3 type transcription factor MYB15 can recognize and bind to the MYB sites on the CBF1/2/3 promoter, inhibit the expression of CBFs and downstream COR genes and is a negative regulator of cold tolerance in *Arabidopsis* and rice [8]. Ectopic expression of *MbDREB1* (belonging to AP2/ERF TFs) from dwarf apple in *Arabidopsis* or *PbCBF1* from peaches in apple significantly enhances the cold tolerance of transgenic plants [9]. Until now, a large number of genes have been identified to play a role in response to LW stress, such as bHLHs, MYBs, DREBs, and NACs [10–13]. However, the mechanism by which these genes respond to cold stress is largely unknown.

Anthocyanins as secondary metabolites that enhance LW stress tolerance by scavenging free radicals and reducing oxidative damage [14, 15]. The biosynthesis of anthocyanins is a branch of the flavonoid biosynthesis pathway. As a direct precursor of anthocyanins biosynthesis, phenylalanine is catalyzed by a series of enzymes and genes to form anthocyanins. This process involves key enzymes such as *PAL* (phenylalanine ammonia-lyase), *C4H* (cinnamate-4-hydroxylase), and *4CL* (4-coumaroyl: CoA-ligase) in the phenylpropanoid biosynthesis pathway. Then, early biosynthetic genes (EBGs) including *CHS* (chalcone synthase), *CHI* (chalcone isomerase), *F3H* (flavonoid 3-hydroxylase), *F3′H* (flavonoid 3'-hydroxylase), *F3′5′H* (flavonoid 3',5'-hydroxylase), and late biosynthetic genes (LBGs) like *DFR* (dihydro flavonol-4-reductase), *LDOX*/*ANS* (leucoanthocyanidin oxygenase/anthocyanin synthase), and *UFGT* (UDP glucose:flavonoid-3-O-glucosyltransferase) are involved in the synthesis process [16, 17]. Low temperatures promote anthocyanin accumulation in apples (M. domestica), rapeseed (*Brassica rapa*), and eggplant (*Solanum melongena*) [17–19]. In addition to the above key enzyme genes, anthocyanin biosynthesis is mainly regulated by a conserved MYB-bHLH-WD40 (MBW) complex. The role of members of this complex, likely MYB and bHLH, in regulating anthocyanin biosynthesis has been certified in a diversity of model plants, that is *Arabidopsis*, maize, and tomato [20–22]. Moreover, mutations at specific sites and genetic manipulation of the bHLH and MYB genes have been shown to enhance anthocyanin accumulation [23, 24]. However, bHLH-interacting genes have not yet been functionally characterized in most plants, especially in perennial forage plants.

Amino acids, as an important small molecule for the synthesis of structural proteins and stress proteins, can be used as osmoprotectant agents to resist LW stress, and can also regulate nitrogen metabolism by increasing the concentration of some amino acids [25, 26]. It is thought that the accumulation of amino acids during stress has a beneficial effect on plants [27]. Proline, a well-known osmotic protectant and molecular chaperone in plants, actively contributes to suppressing reactive oxygen species (ROS), stabilizing protein structures, and maintaining cellular homeostasis [28]. Glutamic acid serves as both a precursor for proline synthesis and a prerequisite for the synthesis of chlorophyll a and chlorophyll b. Therefore, the decrease in glutamic acid content under LW stress may be associated with its utilization for chloroplast biosynthesis in plants to maintain photosynthetic efficiency [29, 30]. The application of foreign amino acids significantly improved the cold resistance of tea plants [31]. Similar changes have

also been observed in wheat [32] and tobacco [28]. In addition, many genes related to amino acid synthesis that respond to LW stress in plants have been identified [33].

Multi-omics analysis is a powerful technique widely employed to elucidate the molecular mechanisms of plant responses to LW stress [34, 35]. Integrated metabolomic and transcriptomic analyses are widely used to study regulatory networks and correlations between genes and metabolites [36, 37]. Furthermore, multi-omics analysis has been effectively applied in the biosynthesis mechanism and gene function identification of secondary metabolites in legumes [1]. However, studies on molecular mechanisms have made few advances in sainfoin response to LW stress. Combined with co-expression analysis of metabolomics and transcriptomics, the molecular mechanism of LW stress in sainfoin was systematically explored, which understand deeply the key genes and metabolic pathways and provides a theoretical basis for the molecular breeding of sainfoin under low-temperature conditions.

2 Materials and methods

2.1 Plant growth condition and stress treatments

The cold-tolerant new line of P4 (9155×*O. viciaefolia* No. 'Gansu', RC) was selected by Gansu Agricultural University, and the cold-sensitive material of 13709 (SC) and cold-tolerant material of 9155 were introduced from Vavilov Plant Gene Bank in Russia.

In the plant growth chamber of Gansu Agricultural University, 1000 g of sterilized sand (121℃, 30 min) was placed in a pot (13.2, 12, 14, and 9.2 cm), after disinfection (75% ethanol, 3% NaClO), distribute the seeds evenly in a flowerpot and cover with sand for 1cm. When the seedlings of outdoor normal cultivation were 50 days old, the disease-free seedlings with consistent growth were selected and placed in an incubator at 25℃ for pretreatment for 24 h, and then placed in a low-temperature incubator at 4℃ for cold treatment, with 20 plants per treatment and 3 biological replicates. As a control, the seedlings of sainfoin without low-temperature treatment were sampled every 12 h, and the maximum cold treatment was 72 h. 6 plants were randomly selected for each sampling, and the leaves of the same parts were taken and snap-frozen in liquid nitrogen and stored in the refrigerator at -80℃ for further use.

2.2 Phenotypic and biochemical measurements

According to Huang et al. the productivity and hydrogen peroxide content of O_2^- were quantified [38]. DAB and NBT were used for histochemical staining to detect in situ O_2^- and H_2O_2 accumulation in leaves [39]. The proline (Pro) and malondialdehyde (MDA) were determined by Chen et al. [40]. Each process is repeated three times.

2.3 Transcriptome sequencing and data analysis

The total RNA of the samples was extracted from the samples after LW stress by Biomarker Cloud Technology Co Ltd (Beijing, China, www.biomarker.com.cn). RNA purity, concentration, and integrity were

assessed using the NanoDrop 2000 Spectrophotometer (Thermo Scientific, USA) and the RNA Nano 6000 Assay Kit of the Agilent Bioanalyzer 2100 (Agilent Technologies, CA, USA), respectively.

After qualifying the library inspection, the cDNA library was sequenced using the Illumina Hiseq high-throughput sequencing platform. After quality control, high-quality Reads were obtained. Trinity software (http://trinityrnaseq.sourceforge.net/; version, number: trinityrnaseq-r2013-02-25) was used for data assembly, and low-expression transcripts were filtered. Finally, unigene and transcript length were counted.

2.4 Transcriptomic analysis

Differential gene expression analysis was performed using DESeq2 [41]. The false discovery rate (FDR) lower than 0.05 and the absolute fold change ≥ 2 were the thresholds for identifying differentially expressed genes (DEGs). Using BLAST software, the annotation information of unigene was obtained and classified by comparing NR, Swiss-Prot, COG, KOG, eggNOG4.5, and KEGG public databases [42]. Compared with the Pfam database, KOBAS2.0 software was used to analyze the KEGG Orthology results of unigene in KEGG, and the amino acid sequence of unigene was predicted, and then HMMER software was used to obtain annotation information [43]. The GO enrichment results of the new genes were analyzed by InterPro software [44]. Expression abundance of the corresponding unigene was expressed using Fragments Per Kilobase of transcript per Million mapped reads (FPKM) values using Bowtie and RSEM (http://deweylab.biostat.wisc.edu/rsem/) [43, 45].

2.5 Metabolites analysis

After low-temperature treatment for 0 and 48 h, 6 repeat samples RC and SC were collected, respectively, and extensive targeted metabolome analysis was performed using a liquid chromatography-mass spectrometry (LC-MS) system provided by Beijing Biomarker Cloud Technology Co Ltd (Beijing, China, www.biomarker.com.cn). LC-MS/MS analysis was performed by Waters Acquity I-Class PLUS ultra-high performance liquid tandem Waters Xevo G2-XS QTof high-resolution mass spectrometer. Next, metabolite identification was based on the following databases: KEGG (http://www.genome.jp/kegg/), HMDB (https://hmdb.ca/), and Lipidmaps (https://lipidmaps.org/). MassLynx V4.2 was used to collect the original data, and Progenesis QI software was used for peak extraction, peak comparison, and other data processing operations. Then, the metabolites were qualitatively and quantitatively based on the METLIN database, public database, and Biomarker's self-built database. Principal Component Analysis (PCA) and orthogonal projections to latent structures-discriminant analysis (PLS-DA) were performed on the data using the metabolomics data processing software MetaboAnalyst 5.0 (https://www.metaboanalyst.ca/MetaboAnalyst/ModuleView.xhtml)), to identify important variables with discernment. The screening criteria for metabolites were Fold Change > 2 or Fold Change < 0.5, *P*-value < 0.05, and VIP > 1. The relative quantitative data of different metabolites were normalized, and the R software was used to cluster the content of different metabolites. KEGG metabolic pathway enrichment analysis was performed.

2.6 Weighted gene co-expression network (WGCN) analysis

Differential genes under LW stress in RC and SC at different time points were used as trait files to generate co-expression networks and modules. The Pearson correlation coefficient was calculated to determine the strength of the relationship between traits and modules. The co-expression network was visualized using Cystoscope (version 3.6.0) [46].

2.7 Joint analysis of transcriptome and metabolome

We analyzed the correlation between transcriptomics and metabolomics data to explore the correlation between DEG and metabolites. The COR function in r was used to calculate the PCC of DEGs and DAMs. Using the genes and metabolites with PCC > 0.8 in the KEGG pathway, a related network visualized by Cystoscope software was established. In addition, the obtained DAMs and DEGs were positioned on the KEGG pathway for integration.

2.8 Verification of candidate genes by quantitative real-time PCR (qRT-PCR)

The same RNA samples for transcriptomics analysis were used in qRT-qPCR experiments. The cDNA was synthesized using the Prime Script TM RT reagent Kit Reverse Transcription Kit (TaKaRa, Dalian, China). cDNA synthesis according to the manufacturer's instructions (TaKaRa, Dalian, China), using DNAMAN software to design primers, and Actin was used as an internal reference gene. Amplification was carried out using Light Cycle® 96 Reat-Time PCR System PCR instrument (Roche Switzerland). The relative expression was calculated by the $2^{-\Delta\Delta Ct}$ method. The primers used for the genes are shown in Supplementary Table S1.

2.9 Statistical analysis

In this experiment, Origin 8.0 software (OriginLab, Hampton, MA, USA) was used for data statistics and mapping. The SPSS version 22.0 (IBM, Armonk, NY, USA) software was used for variance analysis of test data, difference letters above the bars indicated significant difference ($P < 0.05$) as obtained by one-way ANOVA and LSD test.

3 Results

3.1 Phenotypic variation under cold stress

To study the response to LW stress, sainfoin seedlings were exposed to 4℃ for 72 h treatments. LW stress significantly affected the normal growth and development of sainfoin (Fig. 1A). To understand the effect of LW stress on sainfoin, several physiological characteristics between RC and SC were studied. In our research, the content of proline (Pro) in RC was significantly higher than that in SC. Compared with SC, the content of MDA in RC increased significantly. Moreover, the qualitative and quantitative results of O_2^- and H_2O_2 also validate this result (Fig. 1B). These results suggest that RC exhibits better cold resistance.

According to the results of phenotypic and physiological indicators, significant differences were observed between two strains of sainfoin seedlings after 48 h of LW stress. Subsequently, four groups of sainfoin seedlings were prepared for transcriptome and metabolomics analysis: RC 0 h vs SC 0 h, RC 48 h vs SC 48 h, RC 48 h vs RC 0 h, and SC 48 h vs SC 0 h. Each group underwent three independent biological replicates.

3.2 Analysis based on transcriptome data of sainfoin under low-temperature conditions

To analyze the response difference of the two sainfoin varieties to LW stress at the transcriptional level, the global transcriptome profiles of RC and SC were constructed using RNA-seq. Samples were obtained after 0 and 48 h of exposure to 4℃. and the fold change (FC) ≥ 2 and FDR < 0.01 as standard that screened DEGs. According to the PCA, the samples between the groups were scattered, and the samples in the group were clustered (PC1 and PC2) (Fig. 2A). From the transcriptome analysis, 1045, 1412, 5010, and 3119 DEGs were identified from the comparison of RC 0 h vs SC0 h, RC 48 h vs SC 48 h, RC 48 h vs RC 0 h, and SC 48 h vs SC 0 h (Fig. 2B) indicated that the LW stress expanded the difference between the two varieties. A total of 33 core DEGs were consistently identified in both RC and SC at different comparison groups (Fig. 2C and Supplementary Table S2). Hierarchical clustering analysis showed that different strains of sainfoin had different genes that played a regulatory role in response to LW stress (Fig. 2D).

Subsequently, GO analysis revealed DEGs in terms of metabolic process, cells, and cell components as well as catalytic activity (Supplementary Fig. S1). KEGG analysis revealed that a substantial percentage of DEGs were implicated in plant hormone signal transduction, material metabolism (including sugar, protein, lipid, and amino acids, etc.), MAPK signaling pathway, plant-pathogen interaction, glycerophospholipid metabolism, and RNA polymerase (Supplementary Fig. S2).

3.3 Weighted correlation network analysis (WGCNA)

Based on the DEGs obtained from RC and SC transcriptome sequencing, the data were normalized to construct a co-expression network. 12 modules, representing clusters of highly related genes, were generated. Specific modules are depicted with different colors in Fig. 3A. The top 12 modules exhibited cultivar specificity (Fig. 3B). Interestingly, these modules exhibited different expression patterns in RC and SC at different time points (Fig. 3C). A KEGG analysis was conducted on the genes within these modules to determine their associated biological functions. The KEGG enrichment pathways were significantly different among these modules. Importantly, all of these modules were found to be related to the same pathways: plant-pathogen interaction, amino sugar and nucleotide sugar metabolism, phenylpropanoid biosynthesis, and flavonoid biosynthesis (Fig. 3D). These pathways provide valuable insights into the metabolic processes underlying the low temperature of sainfoin. In addition, Hub genes were identified within each module, which can play an essential role in response to LW stress (Fig. 3E).

3.4 The metabolomics analysis of sainfoin revealed the dynamic metabolic spectrum changes under LW stress.

We applied metabolomics based on LC-MS/MS to better understand the metabolic changes of sainfoin during LW stress. As shown in Fig. 4A, the PCA explained 31.0% of the total variance (17.6 and 13.4% for PC1 and PC2, respectively). PCA showed the precise isolation of PC1 between different time points. Genotypes isolated from biological replication can be distinguished by PC2, which showed that there is a good correlation between the repeats (Fig. 4A). Similarly, to better understand the metabolic profile of the LW stress response of red bean grass, we established unsupervised hierarchical clustering, showing that the metabolic data of the control group was significantly separated from LW stress (48 h) (Fig. 4B). Next, cluster analysis was carried out according to its changes in the process of LW stress, and it was divided into 10 clusters according to its changing trend (Fig. 4C-D).

3.5 DAMs involved in LW stress response between two sainfoin

The screening criteria of FC > 1, P < 0.05, and VIP > 1 were used to screen DAMs. To identify the DAMs of sainfoin under LW stress, we compared the number of metabolites in different comparison groups. A total of 6,619 metabolites were detected by untargeted LC-MS analysis, we identified 1056 (443 up and 613 down-regulated) DAMs from the comparison of SC 48 h vs SC 0 h. For the RC, 1125 (691 up and 434 down-regulated) DAMs from RC vs RC 0 h. Another, 859 (381 up-regulated and 478 down-regulated) and 803 (491 up-regulated and 312 down-regulated) DAMs were identified from RC 48 h vs SC 48 h and RC 0 h vs SC 0 h, respectively (Fig. 5A). Notably, we observed an increase in the number of DAMs between the two sainfoin varieties after 48 h of stress time, indicating an active adaptation of the metabolites to LW stress. Nevertheless, relative to the control, the SC has accumulated more metabolites than RC, which indicates the metabolism of SC is disordered after 48 h of LW stress. This data also supports our finding that SC was sensitive to LW stress and RC showed significant tolerance to SC at metabolome levels. The common differential metabolites of the four combinations were shown in the Venn diagram, and 26 core metabolites were identified. Profiles of the 26 common metabolites during different comparison groups can be observed in Fig. 5B and are listed in Supplementary Table S3. What's more, among the core 26 DAMs, the majority reached the peak at RC 48 h. Above-excavated DAMs could mainly categorized into the following categories: lipids and lipid-like molecules, phenylpropanoids and polyketides, organic acids, and other compounds (Fig. 5C).

Another,

3.6 Joint analysis of metabolome and transcriptome data

The changes in DAMs and DEGs in each comparison are visualized using a nine-quadrant graph, where a correlation coefficient value greater than 0.80 is considered. There is a correlation between DAMs and DEGs (Fig. 6A), indicating that metabolites are indirectly or directly regulated by these genes. We integrated DEGs and DAMs into the KEGG pathway and used a threshold value of $P < 0.05$ to screen the

pathways. In these co-mapping pathways, DEGs and DAMs between RC 48 h vs RC 0 h were involved in glycerophospholipid metabolism, flavonoid biosynthesis, glutathione metabolism, and inositol phosphate metabolism were significantly enriched. At the same time, in SC 48 h vs SC 0 h group DEGs and DAMs were involved in monoterpenoid biosynthesis, alpha-linolenic acid metabolism, sphingolipid metabolism, and flavonoid biosynthesis showed high expression. In contrast, DEGs and DAMs between varieties (RC 0 h vs SC 0 h and RC 48 h vs SC48 h) were found to be enriched in cyano amino acid metabolism, fatty acid elongation, ABC transporters, and glucosinolate biosynthesis, galactose metabolism, phenylpropanoid biosynthesis, amino sugar and nucleotide auger metabolism, and pentose and glucuronate interconversions pathways (Fig. 6B).

We found that many DEGs and DAMs were enriched in the same KEGG metabolic pathway in the two sainfoins. These pathways include phenylalanine metabolism, flavonoid biosynthesis, amino acid metabolism et al. (Fig. 6B). More importantly, considering the role of the phenylalanine metabolic biosynthesis pathway in plant disease resistance and stress response, we constructed a correlation network diagram of DEGs and DAMs based on the Pearson correlation coefficient (PCC). As shown in Fig. 7, a total of 42 DEGs and 7 DAMs in the network were highly positively correlated (PCC > 0.8). It is speculated that these genes and metabolites may play an important role in the process of LW of sainfoin.

3.7 Identification of TFs

Transcription factors (TFs), as regulators of gene expression, control the expression of target genes by binding to specific transcriptional regulatory regions, thereby playing a crucial role in plant responses to abiotic stresses. Among these TF families, top of the list are AP2/ERF-ERF, bHLH, MYB, C2H2, MYB-related, and GRAS. It shows that the response of sainfoin to LW stress is a complex multi-factor synergistic regulation process (Fig. 8A). of which 2 TFs were common to both different groups and also showed similar expression patterns (Fig. 8B). Moreover, we investigated the expression levels of AP2/ERF-ERF and bHLH TFs during LW stress, and the expression levels of most of these TFs were induced during LW stress (Fig. 8C-D; Supplementary Table S4,5).

3.8 Biosynthetic pathways associated with anthocyanins in response to LW

DAMs and DEGs produced by LW treatment (RC 48 h and RC 0 h, SC 48 h, and SC 0 h) were enriched in pathways such as the synthesis of flavonoid biosynthesis based on the KEGG analysis (Fig. 6B). Anthocyanin is a secondary metabolite of flavonoids and has powerful scavengers of reactive oxygen species (ROS), which is synthesized by the phenylalanine pathway, early biosynthesis, and late biosynthesis [47]. In total, 7 DAMs were encoded by 26 DEGs located in the anthocyanins synthesis pathway. There are 14 genes strongly up-regulated in 26 genes, including all genes encoding *PAL*, *C4L*, *HCT*, CHS, *F3'H*, and *DFR* (Supplementary Table S10). In the phenylpropanoid biosynthesis pathway, the DEGs of *PAL* (TRINITY_DN14319_c0_g2, TRINITY_DN3446_c0_g1, and TRINITY_DN3446_c0_g2), *4CL* (TRINITY_DN1302_c0_g2, TRINITY_DN9784_c0_g1, TRINITY_DN7939_c0_g1, TRINITY_DN8356_c0_g1,

TRINITY_DN4140_c0_g1, and TRINITY_DN5000_c0_g1), *C4H* (TRINITY_DN14076_c0_g1, TRINITY_DN7964_c0_g1, TRINITY_DN239_c1_g2, and TRINITY_DN17621_c0_g1), and *CSE* (TRINITY_DN4164_c1_g1) were induced, and the corresponding metabolites of caffeic acid significantly changed (Supplementary Table S6-7). The up-regulation DEGs encoding *HCT* (TRINITY_DN1265_c1_g1, TRINITY_DN8377_c0_g1, TRINITY_DN5491_c0_g2, TRINITY_DN4819_c0_g1, and TRINITY_DN16246_c0_g1e) and induced the metabolites of Chlorogenic acid. Cinnamoyl-CoA was catalyzed by *C4H* to form P-Coumaryoyl-CoA. Then, P-Coumaryoyl-CoA was converted to naringenin by a series of enzymes (*CHS*, *CHI*) in the phenylpropanoid biosynthesis pathway. In the latter pathway, naringenin was catalyzed through a series of enzymes, such as *F3H* and *FLS* formed anthocyanin. Since then, (+)-Glalocatechin, 4-Coumaroylshikimate, 4-Hydroxy-3-methoxycinnamic acid, Delphinidin, and Chavicol were induced by the other genes changed (Supplementary Table S7).

3.9 Amino acid metabolism in response to LW stress

To better analyze the synergy between DEGs and DAMs, we also selected DEGs and DAMs related to the amino acid pathway and plotted the difference diagram in sainfoin after LW stress (Fig. 6B). The results showed that 20 significantly different metabolites encoded by 28 markedly DEGs were mapped onto the amino acid biosynthesis pathway (Fig. 10; Supplementary Table S8). In the 28 DEGs, the expression of 18 genes was strongly up-regulated, and 10 genes were strongly down-regulated (Supplementary Table S8). Among them, the DEGs of B16 (TRINITY_DN4859_c0_g1), B17 (TRINITY_DN1848_c0_g2), B18 (TRINITY_DN17856_c0_g1), B19 (TRINITY_DN7147_c0_g2), *FBA* (TRINITY_DN13363_c0_g1), *PGK* (TRINITY_DN6041_c1_g1), *BPGM* (TRINITY_DN10365_c0_g1), *ENO* (TRINITY_DN7739_c0_g1), *PK* (TRINITY_DN48012_c0_g1), B4 (TRINITY_DN44748_c0_g2), B11 (TRINITY_DN7171_c0_g1), B12 (TRINITY_DN6190_c0_g1), and *proA* (TRINITY_DN740_c1_g1, TRINITY_DN19548_c0_g1, TRINITY_DN740_c1_g2, and TRINITY_DN8101_c0_g1) were up-regulated (Supplementary Table S8), and the level of corresponding metabolites of O-Acetylserine markedly increased. Meanwhile, the DEGs of B7 (TRINITY_DN5175_c0_g1), B8 (TRINITY_DN7901_c0_g1), B9 (TRINITY_DN7901_c0_g1), *PBGM* (TRINITY_DN4730_c0_g1 and TRINITY_DN9399_c0_g1), and *PBGM* (TRINITY_DN4730_c0_g1) were down-regulated. In the tricarboxylic acid (TCA pathway), the DEGs of B4 (TRINITY_DN44748_c0_g2), B5 (TRINITY_DN9899_c0_g2), and B6 (TRINITY_DN2370_c0_g1) were up-regulated, and the fumarate metabolite was observed significantly induced due to the B5 changed. And B1(TRINITY_DN4849_c0_g1), B2 (TRINITY_DN5070_c0_g1), B3 (TRINITY_DN3139_c0_g1), and B7 (TRINITY_DN5175_c0_g1) were down-regulated, and B7 was down-regulated caused the (S)-malate significantly changed (Supplementary Table S9). Of note, after LW stress, the metabolites accumulated in RC were redundant to SC, suggesting that RC had higher cold resistance (Supplementary Table S9).

3.10 Gene expression validation by qRT-PCR analysis

To verify the reliability of the transcriptome data, six genes (*CSE* (TRINITY_DN4164_c1_g1), *CHS* (TRINITY_DN17004_c0_g1), *F3H* (TRINITY_DN8693_c0_g1), *DFR* (TRINITY_DN9928_c0_g1), *PGK* (TRINITY_DN6041_c1_g1), and *BPGM* (TRINITY_DN9399_c0_g1)) related to PA synthesis and amino acids biosynthesis were analyzed by qRT-qPCR to validate the RNA-sequencing-based transcriptome

data. Overall, the qRT-PCR results for these target genes exhibited substantial concurrence with the transcriptome analysis outcomes, thereby affirming the precision of the RNA-Seq data.

4 Discussion

4.1 The biosynthetic pathway associated with anthocyanin in the response of sainfoin to LW stress

Anthocyanins have important physiological functions for plant growth and human health, and their synthesis pathway has been widely studied [5]. There is sufficient evidence that LW stimulates anthocyanin accumulation by up-regulating the expression of biosynthetic genes [47, 48]. We observed a significant enrichment of genes involved in the anthocyanin biosynthesis pathway through KEGG analysis (Fig. 6B). Similar to what occurred in apple, *Onobrychis viciifolia*, and *Camellia sinensis* [49–51]. Metabolites are the final products of metabolism, playing substantial physiological and biochemical roles in several plant species under various environmental stresses [31]. Among the identified metabolites related to the anthocyanin synthesis pathway, most of them were enriched in RC. Only the contents of two key metabolites (Delphindin and Chavicol) were focused on SC after LW stress (Supplementary Table S7). This may be the main factor responsible for the difference in low-temperature resistance between RC and SC.

The phenylpropanoid pathway opens the synthesis of plant anthocyanins and *PAL*, *C4H*, and *4CL* are key genes [52, 53]. Simply, L-phenylalanine is catalyzed by *PAL* to produce trans-cinnamic acid and ammonia, which are then converted to 4-coumaroyl-CoA, and then, 4-coumarin acyl-CoA is converted into a variety of compounds such as flavonoids, anthocyanins, and naringenin through a series of catalytic reactions [10]. The current research also confirmed that LW stress induced the expression of genes involved in the phenylpropanoid pathway, such as *PAL* and *4CL*, promoting the adaptation of low-temperature environments [7]. Similar reports occurred in apple, *Brassica rapa*, and maize [10, 17, 21]. In our study, the transcription levels of *PALs*, *C4Hs*, and *4CLs* increased after low-temperature treatment (Fig. 8A; Supplementary Table S5), indicating greater carbon flux into the phenylpropanoid pathway, resulting in increased metabolite accumulation and improved tolerance. These findings are consistent with results from a study on wheat [32]. What's more, 4-coumaroyl shikimate, an intermediate in the lignin synthesis pathway, accumulated in RC but unchanged in SC, confirming the strong resistance of RC. Next, anthocyanins and other flavonoid substances are produced by enzymatic reactions of different branches, including *F3H*, *DFR*, *ANS*, and *UFGT* [54]. Interestingly, these structural genes showed a strong response to LW stress in sainfoin. CHS is a key enzyme in the early stage of the flavonoid biosynthesis pathway, which can induce the expression of *CHI* and *F3H* [55]. In our study, *CHS* and *CHI* genes exhibited higher transcriptional levels after LW treatment compared to before (Fig. 9A; Supplementary Table S6). The expression of *CHI* may be induced by *CHS*, but the specific mechanism needs further study. *F3H* acts on the bifurcation point of the flavonoid pathway, leading to the production of different flavonoids such as flavonoids, anthocyanins, and proanthocyanidins [7]. In the present study, the

expression of F3H was induced by LW treatment, however, its expression levels in RC and SC were different, which may cause the difference in resistance.

DFR catalyzes the reductive reaction of flavonoid-3',5'-hydroxylases to produce anthocyanins, a key step in regulating anthocyanin types. DFR down-regulated inhibit the accumulation of anthocyanins and proanthocyanidins in apples [56]. In grapes, silencing of the DFR gene results in anthocyanin deficiency [57]. In this study, the expression of the downstream gene *DFR* was induced by the upstream genes *CHS*, *CHI*, and *F3H*. Interestingly, the TRINITY_DN21359_c0_g1 (*DFR*) gene was significantly higher than the TRINITY_DN9928_c0_g1 (*DFR*) gene in RC and SC. The observed expression pattern of the DFR gene, along with discussions from relevant previous studies, suggests that differences in gene sequences and promoter regions of these structural genes may be the main reasons for variations in gene function and expression. These differences ultimately impact anthocyanin biosynthesis in the leaves of different strains of sainfoin.

4.2 Role of the amino acid biosynthesis pathway in the response of sainfoin to cold stress

Low temperatures can promote the accumulation of proline and other amino acids, enhancing the cold tolerance of plants [58]. The GO and KEGG enrichment analysis showed that many DAMs and DEGs were related to amino acid metabolism under LW stress (Supplementary Fig. S1-2), which is consistent with previous results reported for tea [31]. Moreover, a total of 17 differential metabolites related to the biosynthesis of amino acids and 28 DEGs were obtained in the present study (Supplementary Table S8-9). Among these differential metabolites, the contents of 12 metabolites were gathered in RC (Supplementary Table S9). This indicates that the amino acid metabolism in cold-tolerant sainfoin is rapid.

The expression of genes related to the amino acid synthesis pathway and the production of metabolites can enhance cold stress resistance in rice and wheat [59, 60]. This study observed an up-regulation in the expression level of the *ProA* gene after LW stress, leading to a significantly higher proline content in RC compared to before treatment. These results are consistent with the findings of our measured physiological indexes (Fig. 10A; Supplementary Table S8). There were no significant differences in DEGs between L-Serine and S-Ribosyl-homocysteine biosynthesis, whereas their expression levels in RC were higher than those in SC (Fig. 10B and Supplementary Table S10). Under LW stress, cold-tolerant tea varieties exhibited significantly higher amino acid accumulation compared to cold-sensitive tea varieties. This enhanced cold resistance may be attributed to the activation of polyamine synthesis and the CBF-COR regulation pathway [61]. Similar regulatory patterns may exist in RC.

The tricarboxylic acid cycle (TCA) can promote ATP synthesis and can also be linked and transformed into other metabolic pathways through metabolic intermediates [62]. Many intermediates from TCA have been shown to play a role in improving plant stress resistance. For example, Previous studies have shown that supplementing with malate can alleviate nutrient deficiency in rice caused by cadmium stress [63]. The accumulation of malate was also detected in tomatoes under cold conditions [64]. In our

study, there were no significant differences in malate between RC and SC; however, the B6 (TRINITY_DN2370_c0_g1) and B7 (TRINITY_DN5175_c0_g1) genes, related to malate synthesis, were induced under LW stress. What's more, studies have found that fumarate can participate in the process of glucose metabolism after degradation as a glucogenic amino acid [65]. The expression of the B5 (TRINITY_DN9899_c0_g2) gene, involved in fumarate synthesis, is significantly higher in RC than in SC, contributing to the higher resistance of RC (Fig. 9 and Supplementary Table S8-9).

4.3 Transcription factors related to cold resistance of sainfoin

Transcription factors play a key role in regulating the expression of plant stress response genes [66]. In the present study, a total of 446 TFs belonging to 20 families were detected. AP2/ERF-ERF and bHLH were the most abundant categories in both RC and SC, comprising 42 and 35 transcripts, respectively (Fig. 8C-D). LW stress significantly induced the expression levels of these DEGs in RC and SC. In addition, we observed that the expression level of TRINITY_DN13789_c0_g1 was up-regulation after LW stress in sainfoin (Supplementary Table S5), and the homologous gene of this gene in *Cicer arietinum* is *ICE1*. Previous studies have demonstrated that the overexpression of the *MdICE1* interacts with *ABI4* to enhance apple cold tolerance [67]. Additionally, it has been found that *MYC67 and MYC70* negatively regulate cold tolerance in *Arabidopsis* by interacting with *ICE1* [68]. Although low temperature induces its expression, the specific regulatory mechanism needs further study. APETALA2/ethylene responsive factor (AP2/EREBP or AP2/ERF) is one of the largest transcription factor families. ERF, which is a subgroup of AP2/ERF, along with other TF families such as WRKY, bHLH, bZIP, MYB, and NAC, enhances cold stress tolerance [69]. For example, a recent study reported that the AP2/ERF-ERF family gene *PtrERF108* regulates raffinose synthesis, thereby positively regulating the cold tolerance of *Poncirus trifoliate* [70]. Furthermore, the homologous gene LOC25481981 (ERF018) of TRINITY_DN7021_c0_g1 in sainfoin was induced by LW stress. Previous studies have demonstrated the *ERF012/018* binds to the (jasmonic acid) JA synthesis promoter and up-regulates the expression of JA synthesis genes, thereby inhibiting the absorption of boron by *Arabidopsis thaliana* [71]. Building upon these findings, it is hypothesized that the AP2/ERF-ERF transcription factors may also play a role in regulating the response of sainfoin to cold stress through the glucose catabolic process.

5 Conclusion

The study compared cold-resistant material P4 (RC) with cold-sensitive 13709 (SC) through physiological, metabolomics, and transcriptomics analyses. It delved into the relationship between gene expression and metabolite biosynthesis, highlighting the importance of anthocyanin and amino acid biosynthesis in sainfoin resistance to LW. This research sheds light on the molecular information for LW resistance in sainfoin. However, further investigation is needed to explore and confirm the key regulatory genes involved in the synthesis pathways and their role in LW stress.

Declarations

Authorship contribution statement:

JC: wrote and revised the manuscript. KW, YH, and SW: analyzed the data. LN: planned and designed the research. All authors read and approved the final manuscript.

Funding:

This work was supported by the National Nature Science Foundation of China (Nos. 32360339); Gansu Science and Technology Plan (Nos: 22YF7NA112), and the Ministry of Finance and Ministry of Agriculture and Rural Affairs: National Modern Agriculture Industry Technology System (CARS-34).

Availability of data and materials

The datasets used and/or analyzed during the current study are available from the corresponding author upon reasonable request.

Ethics approval and consent to participate

Not applicable

Consent for publication

This research has been confirmed for publication in the journal.

Competing interests

The authors have on competing interests

Author details

[1] Key Laboratory of Grassland Ecosystem (Ministry of Education), College of Grassland Science, Gansu Agricultural University, Lanzhou730070, China; Key Laboratory of Forage Germplasm Innovation and New Variety Breeding of Ministry of Agriculture and Rural Affairs (Co-sponsored by Ministry and Province).

References

1. Jin Z, Jiang W, Luo Y, Huang YJ, Yi DX, Pang YZ. Analyses on flavonoids and transcriptome reveals key MYB genes for proanthocyanidins regulation in *Onobrychis Viciifolia*. Front. Plant Sci. 2022; 13:941918. https://doi.org/10.3389/fpls.2022.941918.
2. Fu X, Ji XY, Wang B, Duan L. The complete chloroplast genome of leguminous forage Onobrychis viciifolia. Mitochondrial DNA Part B. 2021; 6:898–899. https://doi.org/10.1080/23802359.2021.1886017.
3. Li Z, Wu Y, Wang R, Liu B, Qian Z, Li C. Assessment of climatic impact on vegetation spring phenology in northern China. Atmosphere. 2023;14:117. https://doi.org/10.3390/atmos14010117.

4. Landi M, Tattini M, Gould KS. Multiple functional roles of anthocyanins in plant-environment interactions. Environ Exp Bot. 2015;119: 4–17. https://doi.org/10.1016/j.envexpbot.2015.05.012.
5. Aslam M, Fakher B, Ashraf MA, Cheng Y, Wang B, Qin Y. Plant low-temperature stress: Signaling and response. Agronomy. 2022; 12:702. https://doi.org/10.3390/agronomy12030702].
6. Kidokoro S, Shinozaki K, Yamaguchi-Shinozaki K. Transcriptional regulatory network of plant cold-stress responses. Trends Plant Sci. 2022: 27; 922–935. https://doi.org/10.1016/j.tplants.2022.01.008.
7. Xie Y, Chen P, Yan Y, Bao C, Li X, Wang L, Shen X. An atypical R2R3 MYB transcription factor increases cold hardiness by CBF-dependent and CBF-independent pathways in apple. New Phytol. 2018: 218: 201–218. https://doi.org/10.1111/nph.14952.
8. Agarwal M, Hao YJ, Kapoor A, Fujil H, Zheng XW, Zhu JK. A R2R3 type MYB transcription factor is involved in the cold regulation of CBF genes and in acquired freezing tolerance. J Biol Chem. 2006; 281:37636–37645. https://doi.org/10.1074/jbc.M605895200.
9. Wisniewski M, Norelli J, Artlip T. Overexpression of a peach CBF gene in apple: a model for understanding the integration of growth, dormancy, and cold hardiness in woody plants. Front plant Sci. 2015; 6: 85. https://doi.org/10.3389/fpls.2015.00085.
10. Xie XB, Li S, Zhang RF, Zhao J, Chen YC, Zhao Q, Hao Y J. The bHLH transcription factor MdbHLH3 promotes anthocyanin accumulation and fruit colouration in response to low temperature in apples. Plant Cell Environ. 2012;35:1884–1897. https://doi.org/10.1111/j.1365-3040.2012.02523.x.
11. An JP, Wang XF, Zhang XW, Xu HF, Bi SQ, You CX, Hao YJ. An apple MYB transcription factor regulates cold tolerance and anthocyanin accumulation and undergoes MIEL1-mediated degradation. Plant Biotechnol J. 2020; 18:337–353. https://doi.org/10.1111/pbi.13201.
12. Mei C, Yang J, Mei Q, Jia D, Yan P, Feng B, Ma FW. MdNAC104 positively regulates apple cold tolerance via CBF-dependent and CBF-independent pathways. Plant Biotechnology J. 2023; 21:2057–2073. https://doi.org/10.1111/pbi.14112.
13. Wang J, Lian W, Cao Y, Wang X, Wang G, Qi C, Guo YD. Overexpression of BoNAC019, a NAC transcription factor from Brassica oleracea, negatively regulates the dehydration response and anthocyanin biosynthesis in *Arabidopsis*. Sci Rep. 2018; 8:13349. https://doi.org/10.1038/s41598-018-31690-1.
14. Wang B, Wu C, Wang G, He J, Zhu S. Transcriptomic analysis reveals a role of phenylpropanoid pathway in the enhancement of chilling tolerance by pre-storage cold acclimation in cucumber fruit. Sci Hortic-Amsterdam. 2021; 288:110282. https://doi.org/10.1016/j.scienta.2021.110282.
15. Jin HX, Jiang M, Yang JF, Wu ZH, Ma LL, Wang CC, Liang C. A survey of enhanced cold tolerance and low-temperature-induced anthocyanin accumulation in a Novel Zoysia japonica biotype. Plants. 2022; 11:429. https://doi.org/10.3390/plants11030429.
16. Zhang JY, Luo W, Zhao Y, Xu YY, Song SH, Chong K. Comparative metabolomic analysis reveals a reactive oxygen species-dominated dynamic model underlying chilling environment adaptation and tolerance in rice. New Phytol. 2016; 211:1295–1310. https://doi.org/10.1111/nph.14011.

17. Ahmed NU, Park JI, Jung HJ, Hur Y, Nou IS. Anthocyanin biosynthesis for cold and freezing stress tolerance and desirable color in Brassica rapa. Funct Integr Genomic. 2015; 15:383–394. https://doi.org/10.1007/s10142-014-0427-7.
18. XieXB, Li S, Zhang RF, Zhao J, Chen YC, Zhao Q, Yao YX, You CX, Zhang XS, Hao YJ. The bHLH transcription factor *MdbHLH3* promotes anthocyanin accumulation and fruit colouration in response to low temperature in apples. Plant Cell Environ. 2012; 35:1884–1897. https://doi.org/10.1111/j.1365-3040.2012.02523.x.
19. Zhou L, He Y, Li J, Liu Y, Chen H. CBFs function in anthocyanin biosynthesis by interacting with *MYB113* in eggplant (*Solanum melongena* L.). Plant Cell Physiol. 2020;61: 416–426. https://doi.org/10.1093/pcp/pcz209.
20. Qi TC, Song SS, Ren QC, Wu DW, Huang H, Chen Y, Fan M, Peng W, Ren C, Xie DX. The Jasmonate-ZIM-domain proteins interact with the WD-Repeat/bHLH/MYB complexes to regulate Jasmonate-mediated anthocyanin accumulation and trichome initiation in *Arabidopsis thaliana*. The Plant Cell. 2011; 23:1795–1814. https://doi.org/10.1105/tpc.111.083261.
21. Pei L, Liu J, Zhou Y, Jiang Y, Li H. Transcriptomic and metabolomic profiling reveals the protective role of anthocyanins in alleviating low phosphate stress in maize. Physiol Mol Biol Pla. 2021; 27:889–905. https://doi.org/10.1007/s12298-021-00981-9.
22. Kang SI, Rahim MA, Afrin KS, Jung HJ, Kim HT, Park JI. Expression of anthocyanin biosynthesis-related genes reflects the peel color in purple tomato. Hortic Environ Biote. 2018;59:435–445. https://doi.org/10.1007/s13580-018-0046-7.
23. Gao-Takai M, Katayama-Ikegami A, Matsuda K, Shindo H, Uemae S, Oyaizu M. A low temperature promotes anthocyanin biosynthesis but does not accelerate endogenous abscisic acid accumulation in red-skinned grapes. Plant Sci. 2019; 283:165–176. https://doi.org/10.1016/j.plantsci.2019.01.015.
24. Kovinich N, Arnason JT, De Luca V, Miki B. Coloring soybeans with anthocyanins. The Biological Activity of Phytochemicals. 2011: 47–57. https://doi.org/10.1007/978-1-4419-7299-6_4.
25. Xu GX, Li LJ, Zhou J, He MQ, Lyu D, Zhao DY, Qin SJ. Integrated transcriptomics and metabolomics analyses reveal key genes and essential metabolic pathways for the acquisition of cold tolerance during dormancy in apple. Environ Exp Bot. 2023:105413. https://doi.org/10.1016/j.envexpbot.2023.105413.
26. Xu Q, Fan N, Zhuang L, Yu J, Huang B. Enhanced stolon growth and metabolic adjustment in cree bentgrass with elevated CO_2 concentration. Environ Exp Bot. 2018;155:87–97. https://doi.org/10.1016/j.envexpbot.2018.06.027.
27. Xu JD, Yan JJ, Li WJ, Wang QY, Wang CX, Guo JX, Geng DL, Guan QM, Ma FW. Integrative analyses of widely targeted metabolic profiling and transcriptome data reveals molecular insight into metabolomic variations during apple (*Malus domestic*a) fruit development and ripening. Int J Mol Sci. 2020; 21:4797. https://doi.org/10.3390/ijms21134797.

28. Aghdam MS, Moradi M, Razavi F, Rabiei V. Exogenous phenylalanine application promotes chilling tolerance in tomato fruits during cold storage by ensuring the supply of NADPH for activation of ROS scavenging systems. Sci. Hortic. 2019; 246:818–825. https://doi.org/10.1016/j.scienta.2018.11.074 (2019).
29. Kumari A, Parida AK. Metabolomics and network analysis reveal the potential metabolites and biological pathways involved in salinity tolerance of the halophyte Salvadora persica. Environ Exp Bot. 2018;148:85–99. https://doi.org/10.1016/j.envexpbot.2017.12.021.
30. Mokochinski JB, Mazzafera P, Sawaya ACHF, Mumm R, De Vos RCH, HallRD. Metabolic responses of Eucalyptus species to different temperature regimes. J Integr Plant Biol. 2018; 60:397–411. https://doi.org/10.1111/jipb.12626.
31. Zhu X, Liao J, Xia X, Xiong F, Li Y, Shen J, Wen B, Ma Y, Wang Y, Fang W. Physiological and iTRAQ-based proteomicanalyses reveal the function of exogenous γ-aminobutyric acid (GABA) in improving tea plant (*Camellia sinensis* L.) tolerance at cold temperature. BMC Plant Biol. 2019; 19: 43. https://doi.org/10.1186/s12870-019-1646-9.
32. Lv LJ, Dong C, Liu YP, Zhao AJ, Zhang YL, Li H, Chen XY. Transcription-associated metabolomic profiling reveals the critical role of frost tolerance in wheat. BMC Plant Biology. 2022; 22:1–22. https://doi.org/10.1186/s12870-022-03718-2.
33. Zhang QF, Liu MY, Ruan JY. Metabolomics analysis reveals the metabolic and functional roles of flavonoids in light-sensitive tea leaves. BMC Plant Biol. 2017; 17:64. https://doi.org/10.1186/s12870-017-1012-8.
34. Raza A, Su W, Hussain MA, Mehmood SS, Zhang XK, Cheng Y, Zou XL, Lv Y. Integrated analysis of metabolome and transcriptome reveals insights for cold tolerance in rapeseed (*Brassica napus* L.). Front Plant Sci. 2021;12: 721681. https://doi:10.3389/fpls.2021.721681.
35. Lee JH, Kwon MC, Jung ES, Lee CH, Mvuna-Min O. Physiological and metabolomic responses of kale to combined chilling and UV-A treatment. Int J Mol Sci. 2019; 20:4950. https://doi.org/10.3390/ijms20194950.
36. Zhao X, Chen MJ, Li ZP, Zhao Y, Yang HL, Zha L, Yu CX, Wu YJ, Song XX. The response of Volvariella volvaceato low-temperature stress based on metabonomics. Front Microbiol. 2020; 11:1787. https://doi.org/10.3389/fmicb.2020.01.
37. Jian HJ, Xie L, Wang YH, Cao YH, Wan MY, Lv DQ, Li JN, Lu K, Xu XF, Liu LZ. Characterization of cold stress responses in different rapeseed ecotypes based on metabolomics and transcriptomics analyses. Peer J. 2020;8. https://doi:10.7717/peerj.8704.
38. Huang XS, Wang W, Zhang Q, Liu J H. A basic helix-loop-helix transcription factor, *PtrbHLH*, of Poncirus trifoliata confers cold tolerance and modulates peroxidase-mediated scavenging of hydrogen peroxide. Plant Physiol. 2013; 162:1178–1194. https://doi.org/10.1104/pp.112.210740.
39. Romero-Puertas MC, Rodríguez-Serrano M, Corpas FJ, Gómez MD, DelRíoLA, Sandalio LM. Cadmium-induced subcellular accumulation of O_2^- and H_2O_2 in pea leaves. Plant Cell Environ. 2021;204:1122–1134. https://doi:10.1111/j.1365-3040.2004.01217x.

40. Chen YE, Cui JM, Li GX, Yuan M, Zhang ZW. Effect of salicylic acid on the antioxidant system and photosystem II in wheat seedlings. Biol Plant. 2016; 60:139–147. https://doi.org/10.1007/s10535-015-0564-4.
41. Love MI, Huber W, Anders S. Moderated estimation of fold change and dispersion for RNA-seq data with DESeq2. Genome Biology. 2014; 15: 550. https://doi.org/10.1186/s13059-014-0550-8.
42. Li B, Dewey CN. RSEM: accurate transcript quantification from RNA-Seq data with or without a reference genome. BMC Bioinformatics. 2011; 12:1–16. https://doi.org/10.1186/1471-2105-12-323.
43. Xie C, Mao XZ, Huang JJ, Ding Y, Wu JM, Dong S, Kong L, Gao G, Li CY, Wei LP. KOBAS 2.0: a web server for annotation and identification of enriched pathways and diseases. Nucleic Acids Res. 2011; 39: W316–322. https://doi.org/10.1093/nar/gkr483.
44. Rex R. The Gene ontology resource: enriching a gold mine. Nucleic acids research. 2021;49: D325–D334. https://doi.org/10.1093/nar/gkaa1113.
45. Langmead B, Trapnell C, Pop M, Salzberg SL. Ultrafast and memory-efficient alignment of short DNA sequences to the human genome. Genome biology. 2009; 10: 1–10. https://doi.org/10.1186/gb-2009-10-3-r25.
46. Paul S, Andrew M, Owen O, Nitin SB, Jonathan TW, Daniel R, Cytoscape: a software environment for integrated models of biomolecular interaction networks. Genome Res. 2003;13:2498–2504. https://doi:10.1101/gr.1239303.
47. Federica G, Chiara P, Ilaria F, Lorenzo L, Nicola B, Diego T. Low night temperature at veraison enhances the accumulation of anthocyanins in corvina grapes (*Vitis Vinifera* L.). Sci Rep. 2018; 8: 8719. https://doi.org/10.1038/s41598-018-26921-4.
48. Jogawat A, Yadav B, Chhaya-Lakra N, Singh AK, Narayan OP. Crosstalk between phytohormones and secondary metabolites in the drought stress tolerance of crop plants: A review. Physiol Plant. 2021; 5: 1106–1132. https://doi:10.1111/ppl.13328.
49. An JP, Wang XF, Zhang XW, You CX, Hao Y J. Apple Bbox protein BBX37 regulates jasmonic acid mediated cold tolerance through the JAZ-BBX37-ICE1-CBF pathway and undergoes MIEL1-mediated ubiquitination and degradation. New Phytol. 2020; 229:2707–2729. https://doi:10.1111/nph.17050.
50. Thill J, Regos I, Farag MA, Ahmad AF, Kusek J, Castro A, Schlangen K, Carbonero CH, Gadjev IZ. Polyphenol metabolism provides a screening tool for beneficial effects of *Onobrychis viciifolia* (sainfoin). Phytochemistry. 2012; 82: 67–80. https://doi.org/10.1016/j.phytochem.2012.05.030.
51. Jiang X, Huang K, Zheng G. Hou H, Wang P, Jiang H, Zhao X, Li M, Zhang S, Liu Y, Gao L, Zhao L, Xia T. CsMYB5a and CsMYB5e from Camellia sinensis differentially regulate anthocyanin and proanthocyanidin biosynthesis. Plant Sci. 2017; 270: 209–220. https://doi:10.1016/j.plantsci.2018.02.009.
52. Dong NQ, Lin HX. Contribution of phenylpropanoid metabolism to plant development and plant-environment interactions. J Integr Plant Biol. 2021; 63; 180–209. https://doi.org/10.1111/jipb.13054.

53. Li X, Zhang LP, Zhang L, Peng Y, Ahammed GJ, Han WY. Methyl salicylate enhances flavonoid biosynthesis in tea leaves by stimulating the phenylpropanoid pathway. Molecules. 2019;24; 362. https://doi.org/10.3390/molecules24020362.
54. Li Z, Ahammed GL. Hormonal regulation of anthocyanin biosynthesis for improved stress tolerance in plants. Plant Physiol Bioch. 2023:107835. https://doi.org/10.1016/j.plaphy.2023.107835.
55. Czemmel S, Heppel SC, Bogs J. R2R3 MYB transcription factors: key regulators of the flavonoid biosynthetic pathway in grapevine. Protoplasma. 2012;249:109–118. https://doi.org/10.1007/s00709-012-0380-z.
56. Li H, Flachowsky H, Fischer TC, Hanke MV, Forkmann G, Treutter D, Szankowski I. Maize Lc transcription factor enhances biosynthesis of anthocyanins, distinct proanthocyanidins, and phenylpropanoids in apple (*Malus domestica Borkh.*). Planta. 2007;226: 1243–1254. https://doi.org/10.1007/s00425-007-0573-4.
57. Terrier N, Torregrosa L, Ageorges A, Vialet S, Verries C, Cheynier V, Romieu C. Ectopic expression of *VvMybPA2* promotes proanthocyanidin biosynthesis in grapevine and suggests additional targets in the pathway. Plant Phy. 2009; 149:1028–1041. https://doi.org/10.1104/pp.108.131862.
58. Bao YY, Meng N, Wang J, Fu D, Wang L, Cang JJ. The adaptability of winter wheat Dongnongdongmai 1 (*Triticum aestivum* L.) to overwintering in alpine regions. Plant biology. 2021: 23. https://doi:10.1111/plb.13200.
59. Xian L, Tian JQ, Long YX, Ma HJ, Tian M, Liu XD, Yin GY, Wang L. Metabolomics and transcriptomics analyses provide new insights into the nutritional quality during the endosperm development of different ploidy rice. Front. Plant Sci. 2023; 14:1210134. https://doi:10.3389/fpls.2023.1210134.
60. Cheng G, Zhang L, Wang H, Lu J, Wei H, Yu S. Transcriptomic profiling of young cotyledons response to chilling stress in two contrasting cotton (*Gossypium hirsutum* L.) genotypes at the seedling stage. Int J Mol Sci. 2020; 21:5095. https://doi.org/10.3390/ijms21145095.
61. Cheng YH, Ban QY, Mao JL, Lin ML, Zhu XX, Xia YH, Cao XJ, Zhang XC, Li YY. Integrated metabolomic and transcriptomic analysis reveals that amino acid biosynthesis may determine differences in cold-tolerant and cold-sensitive tea cultivars. Int. J. Mol. Sci. 2023; 24:1907. https://doi.org/10.3390/ijms24031907.
62. Wang L, Liu Y, Zhao HY, Zheng YB Bai F, Deng SC, Chen ZX, WU JW, Liu XD. Identification of qGL3.5, a novel locus controlling grain length in rice through bulked segregant analysis and fine mapping. Front. Plant Sci. 2022; 13:921029. https://doi:10.3389/fpls.2022.921029.
63. Sebastian A, Prasad MNV. Exogenous citrate and malate alleviate cadmium stress in Oryza sativa L.: Probing role of cadmium localization and iron nutrition. Ecotox. Environ. Safe. 2018;166:215–222. https://doi.org/10.1016/j.ecoenv.2018.09.084.
64. Zhang WF. Integrative comparative analyses of metabolite and transcript profles uncovers complex regulatory network in tomato (*Solanum lycopersicum* L.) fruit undergoing chilling injury. Sci. Rep. 2019; 9:13. https://doi.org/10.1038/s41598-019-41065-9.

65. Xu J, Chen Z, Wang F, Jia W, Xu Z. Combined transcriptomic and metabolomic analyses uncover rearranged gene expression and metabolite metabolism in tobacco during cold acclimation. Sci Rep. 2020; 10:5242. https://doi.org/10.1038/s41598-020-62111-x.
66. Zhou Q, Luo D, Chai X, Wu Y, Wang YR, Nan ZB, Yang QC, Liu WX, Liu ZP. Multiple regulatory networks are activated during cold stress in *Medicago sativa* L. J Mol Model. 2018; 19:3169. https://doi.org/10.3390/ijms19103169.
67. An JP, Xu RR, Liu X, Su L, Yang K, Wang XF, Wang GL, You CX. ABI4 interacts with ICE1 and JAZ proteins to regulate abscisic acid signaling-mediated cold tolerance in apple. J. Exp. Bot. 2021:10. https://doi.org/10.1093/jxb/erab433.
68. Ohta ML, Sato AL, Renhu NL, Yamamoto TL, Oka NL, Zhu JKL, Tada YL, Suzaki T, Miura K. MYC-type transcription factors, *MYC67* and *MYC70*, interact with ICE1 and negatively regulate cold tolerance in *Arabidopsis*. Sci Rep-uk. 2018:8. https://doi.org/10.1038/s41598-018-29722-x.
69. Feng K, Hou XL, Xing GM, Liu JX, Duan AQ, Xu ZS, Li MY, Zhuang J. Advances in AP2/ERF super-family transcription factors in plant. Crit Rev Biotechnol. 2021; 9:750–776. https://doi:10.1080/07388551.2020.1768509.
70. Khan M, Hu JB, Dahro B, Ming R, Zhang Y, Wang Y, Alhag A, Li CL, Liu LH. ERF108 from *Poncirus trifoliata* (L.) Raf. functions in cold tolerance by modulating raffinose synthesis through transcriptional regulation of *PtrRafS*. Plant J. 2021; 11:705–724. https://doi:10.1111/tpj.15465.
71. Huang Y, Wang S, Wang C, Ding GD, Cai HM, Shi L, Xu FS. Induction of jasmonic acid biosynthetic genes inhibits Arabidopsis growth in response to low boron. J Integr Plant Biol. 2021; 63:937–948. https://doi.org/10.1111/jipb.13048.

Figures

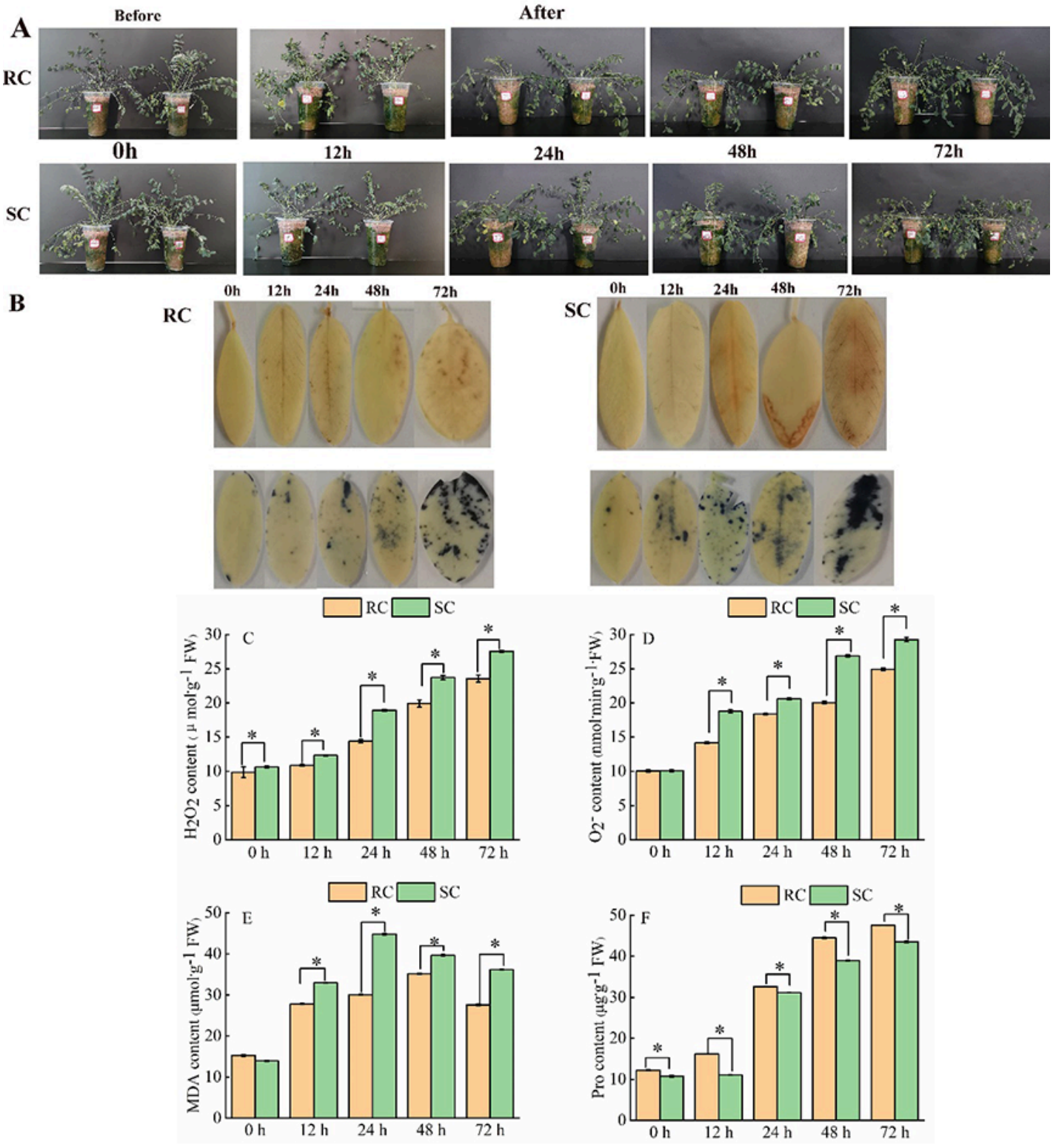

Figure 1

Physiological indexes of sainfoin under LW stress. (A) Shoot morphology. (B) H_2O_2 staining and $O_2^{\cdot}$ staining. (C) The content of H_2O_2. (D)The content of $O_2^{\cdot-}$. (E) MDA content; (F) Pro content. RC: cold-tolerant new line of P4; SC: cold-sensitive material of 13709.

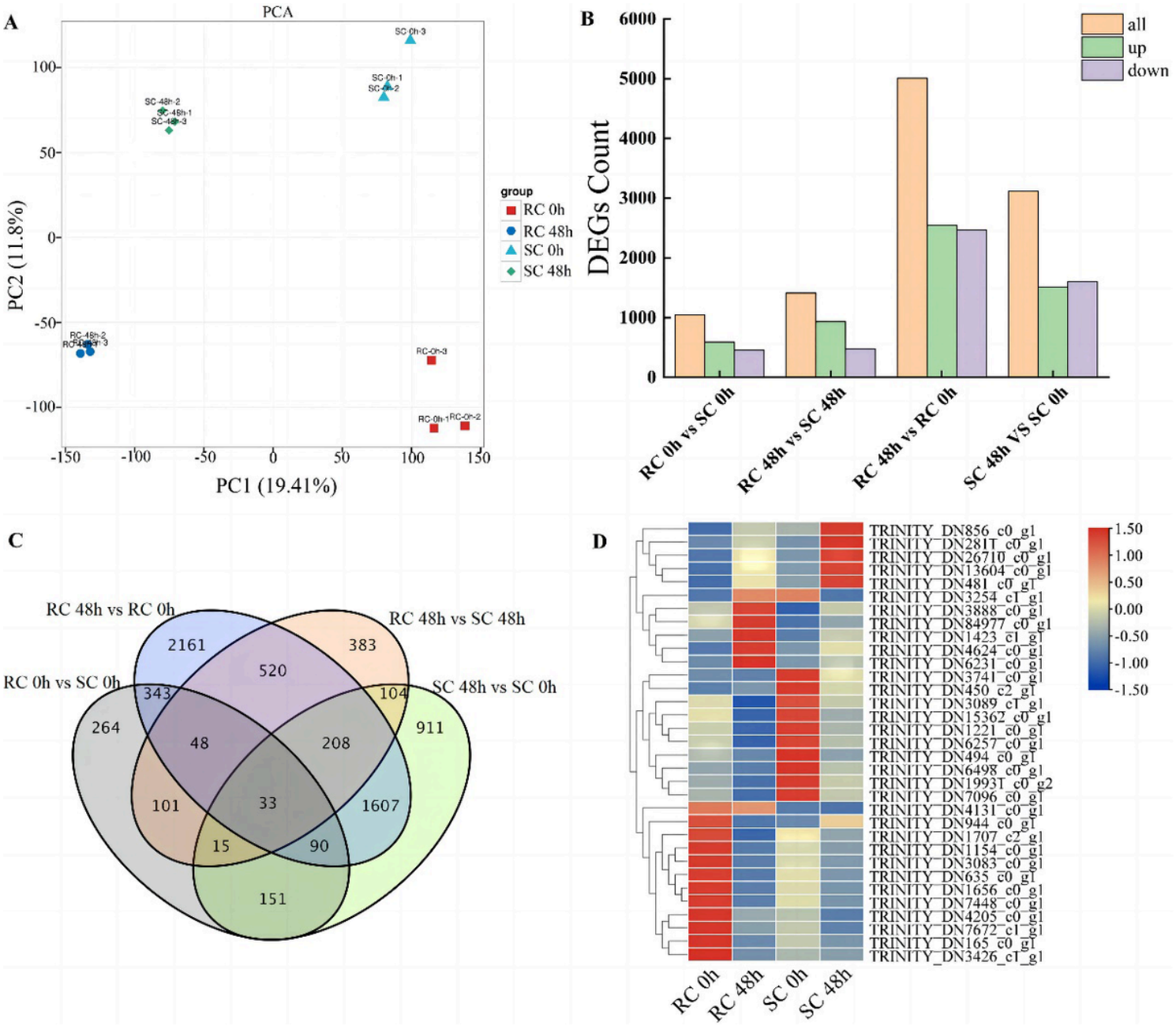

Figure 2

Correlation and PCA analysis of all transcripts and identification of DEGs. (A) PCA plot of transcriptome results. (B)Numbers of DEGs between different comparisons (C) Venn diagram of DEGs among 4 comparison groups (FDR < 0.01 and FC ≥2). (D) Hierarchical clustering of core key DEGs. RC: cold-tolerant new line of P4; SC: cold-sensitive material of 13709.

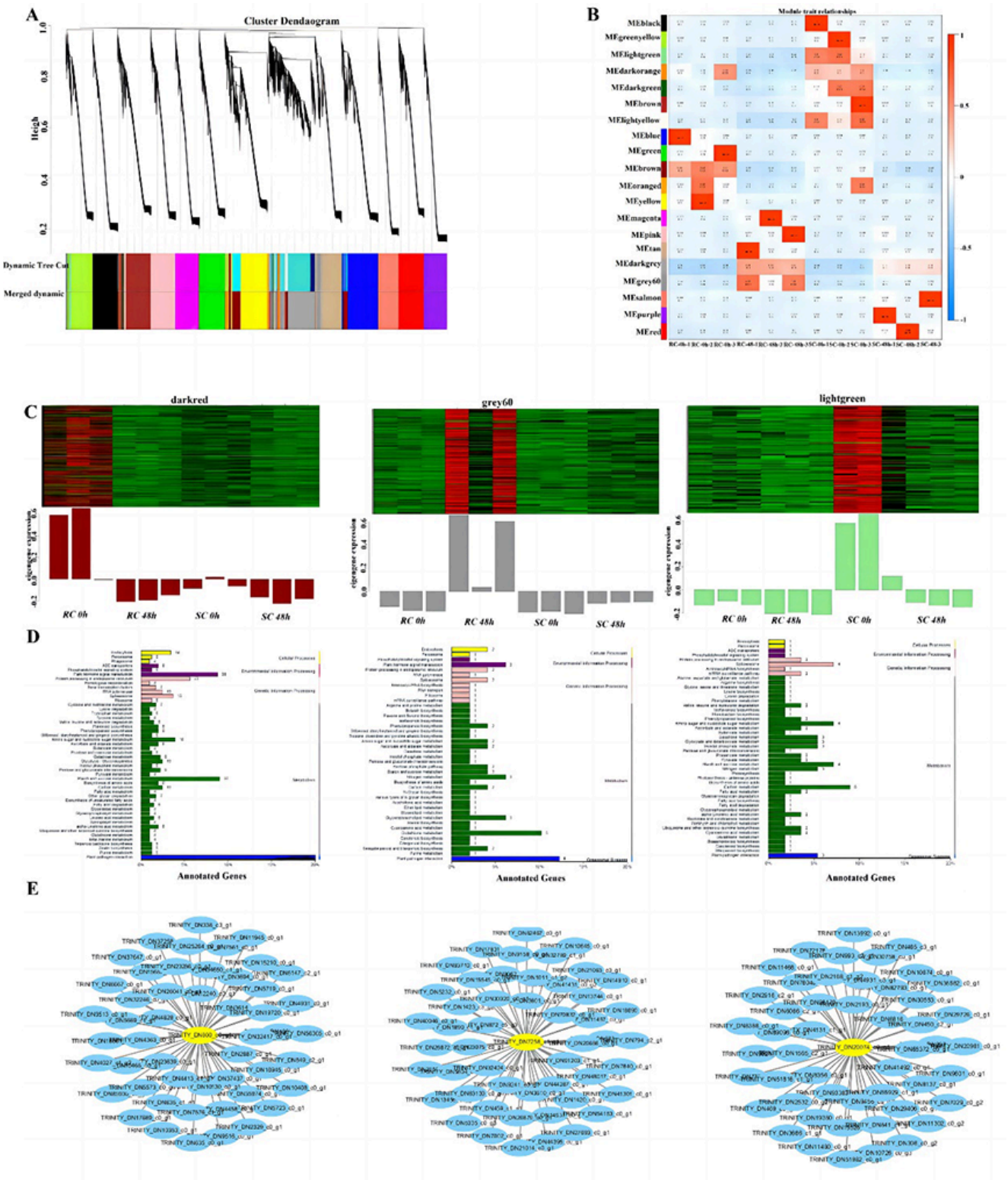

Figure 3

Weighted gene co-expression network (WGCNA) analysis of the DEGs of sainfoin. (A) Cluster dendrogram of 12 expression modular. (B) Module-trait relationships. (C) Expression heat map and expression levels of genes in the module. (D) KEGG enrichment analysis of genes in the modular. (E): Correlation networks of hub genes corresponding to the modular. RC: cold-tolerant new line of P4; SC: cold-sensitive material of 13709.

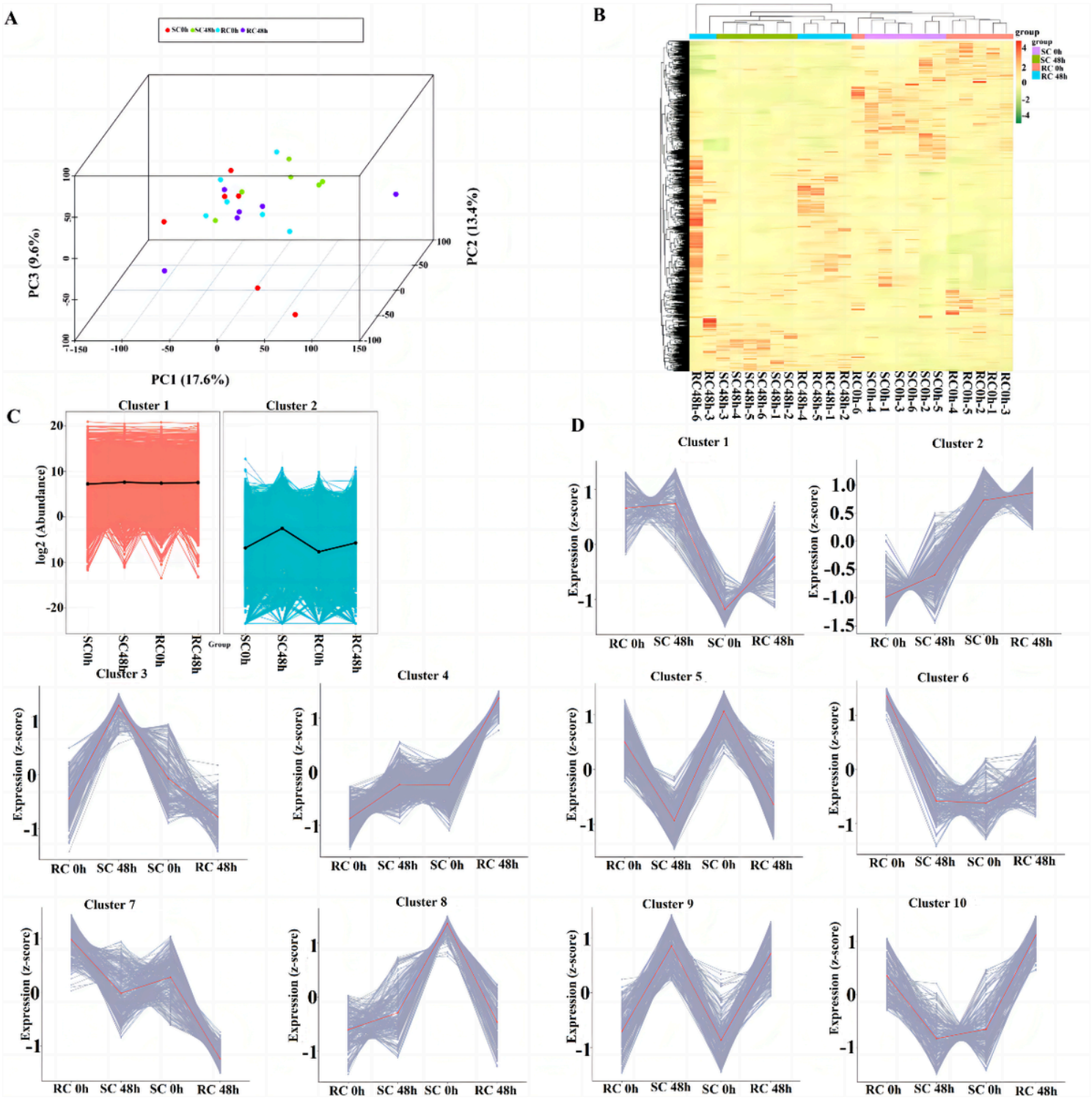

Figure 4

The dynamic metabolome of sainfoin under LW stress. (A) Principal component analysis (PCA) of the LW stress process. (B) Heat map of all metabolites under LW stress. Color represents the relative content level of each DAM, from green low) to red (high). (C) The variation trend of Keanm cluster analysis of metabolites during LW stress of sainfoin. (D) Cluster analysis was performed on the trend of DAMs during LW stress of sainfoin.

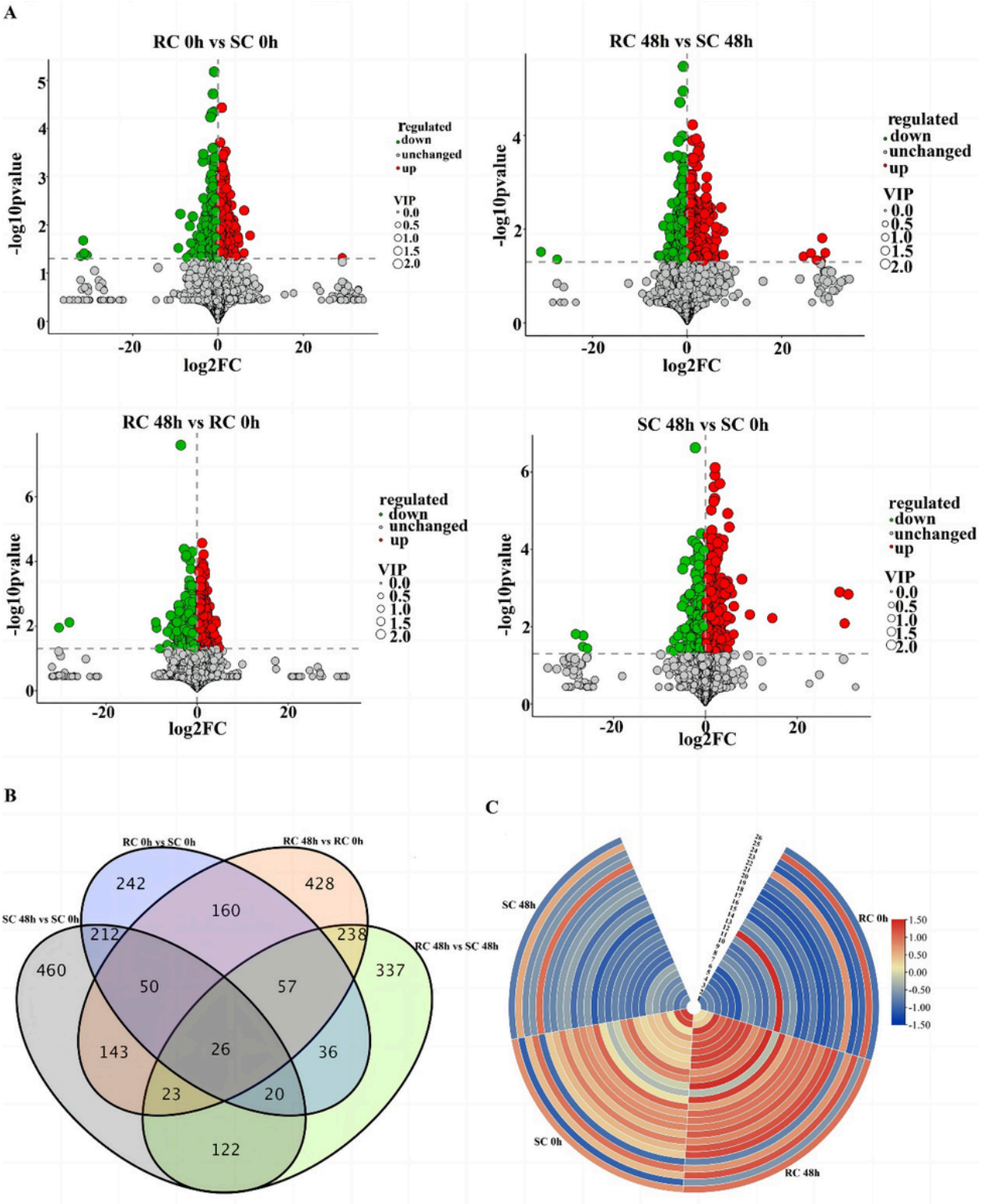

Figure 5

Differentially accumulated metabolites in sweet cherry at different fruit development stages. (A) Volcano plots of differential metabolites in RC 0 h vs. SC 0 h, RC 48 h vs SC 48 h, RC 48 h vs RC 0 h, and SC 48 h vs SC 0 h, respectively. (B) Venn diagram of DEMs in the above four comparison groups. (C) Heatmap of 26 DEMs obtained from the intersection of the comparison group.

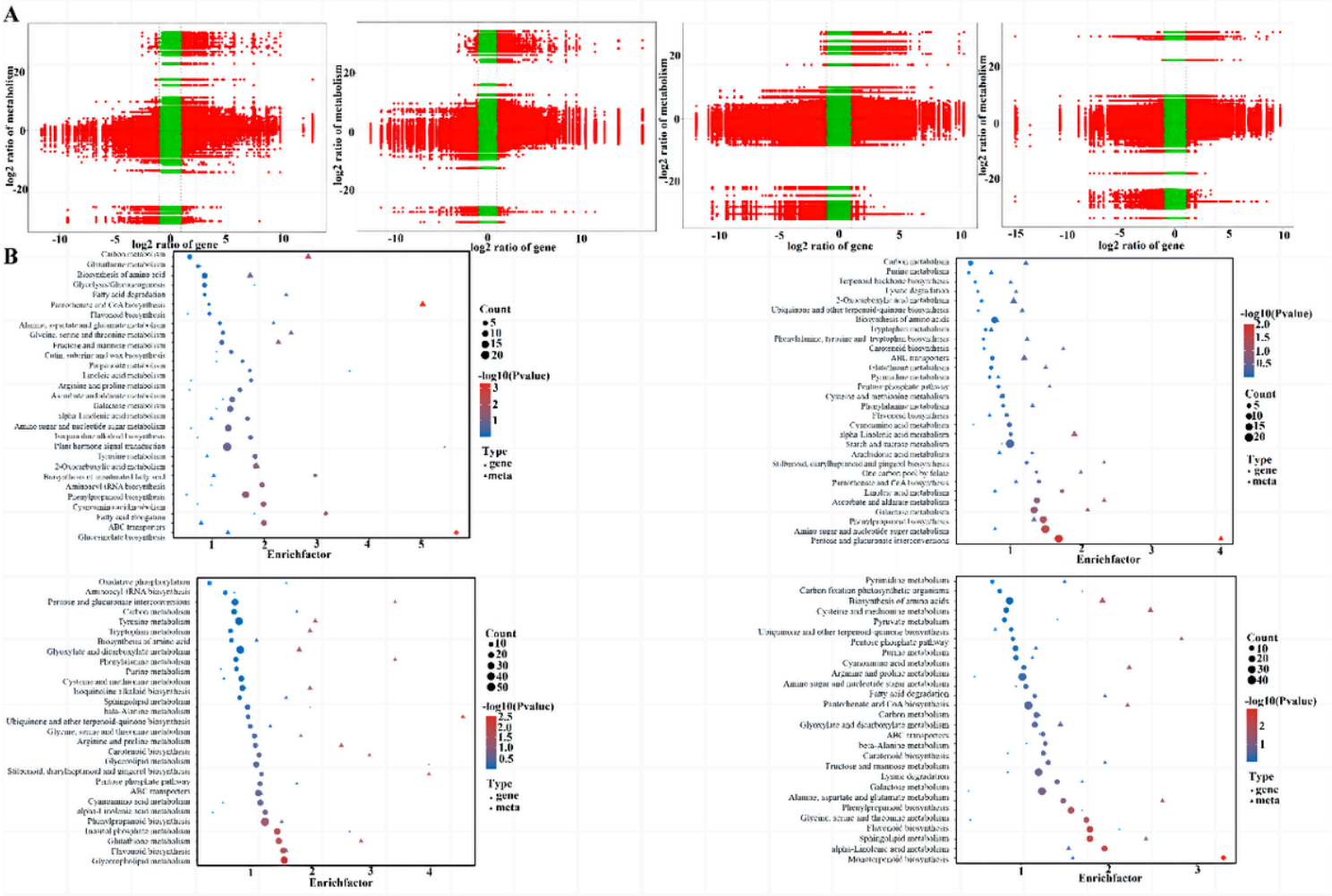

Figure 6

Correlation analysis of metabolomic and transcriptomic data. (A) Nine-quadrant diagrams show the correlation of compounds (obtained from metabolomic analysis) and genes (identified from RNA-seq) in sainfoin (B) KEGG pathway enrichment analysis of genes and metabolism in RC 0 h vs SC 0 h, RC 48 h vs SC 48 h, RC48 h vs RC 0 h, and SC 48 h vs SC 0 h. RC: cold-tolerant new line of P4; SC: cold-sensitive material of 13709.

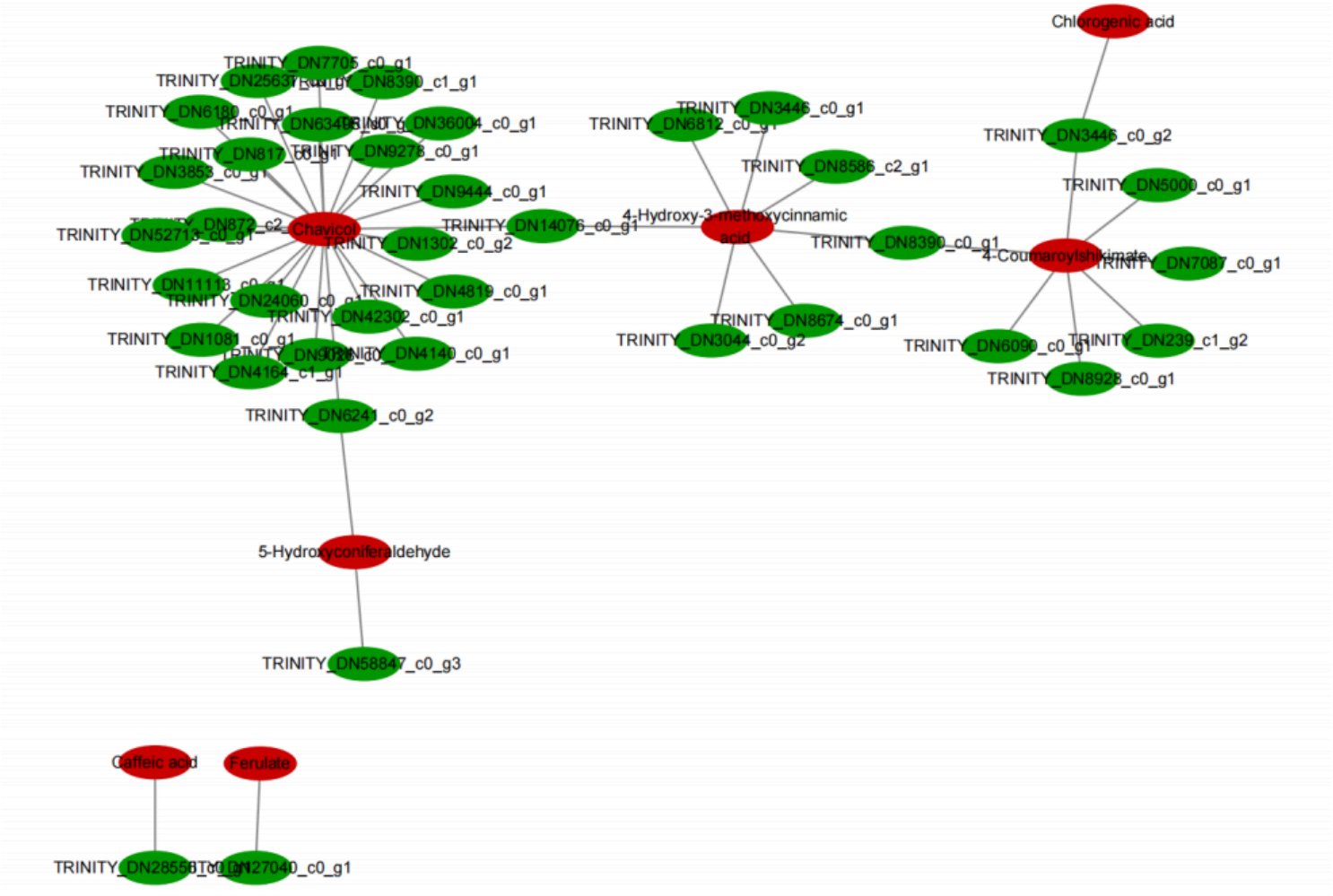

Figure 7

Connection network between DEGs and differentially accumulated metabolites in phenylpropanoid biosynthesis pathway. Metabolites were marked red, structural genes were green.

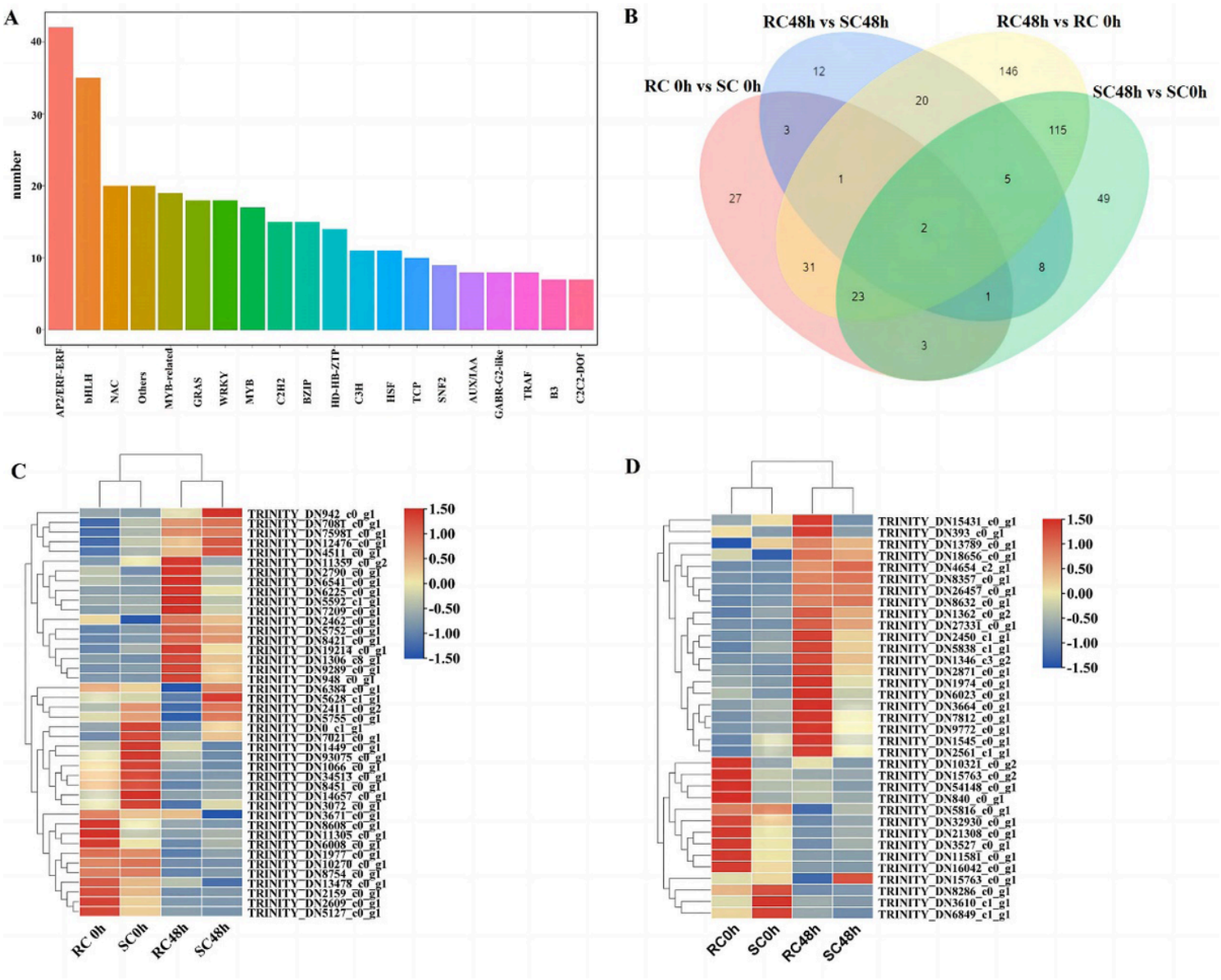

Figure 8

Review of transcription factors in DEGs. (A) Distribution of transcription factors in cold-resistant and cold-sensitive materials DEGs under LW stress. (B) Venn diagram showing TFs among the DEGs in different groups. (C) Heat maps of AP2/ERF-ERF transcription factors identified in DEGs. (D) Heat maps of bHLH transcription factors identified in DEGs. Orange, red, and light blue in the heat map represent the expression levels of transcription factors. RC: cold-tolerant new line of P4; SC: cold-sensitive material of 13709.

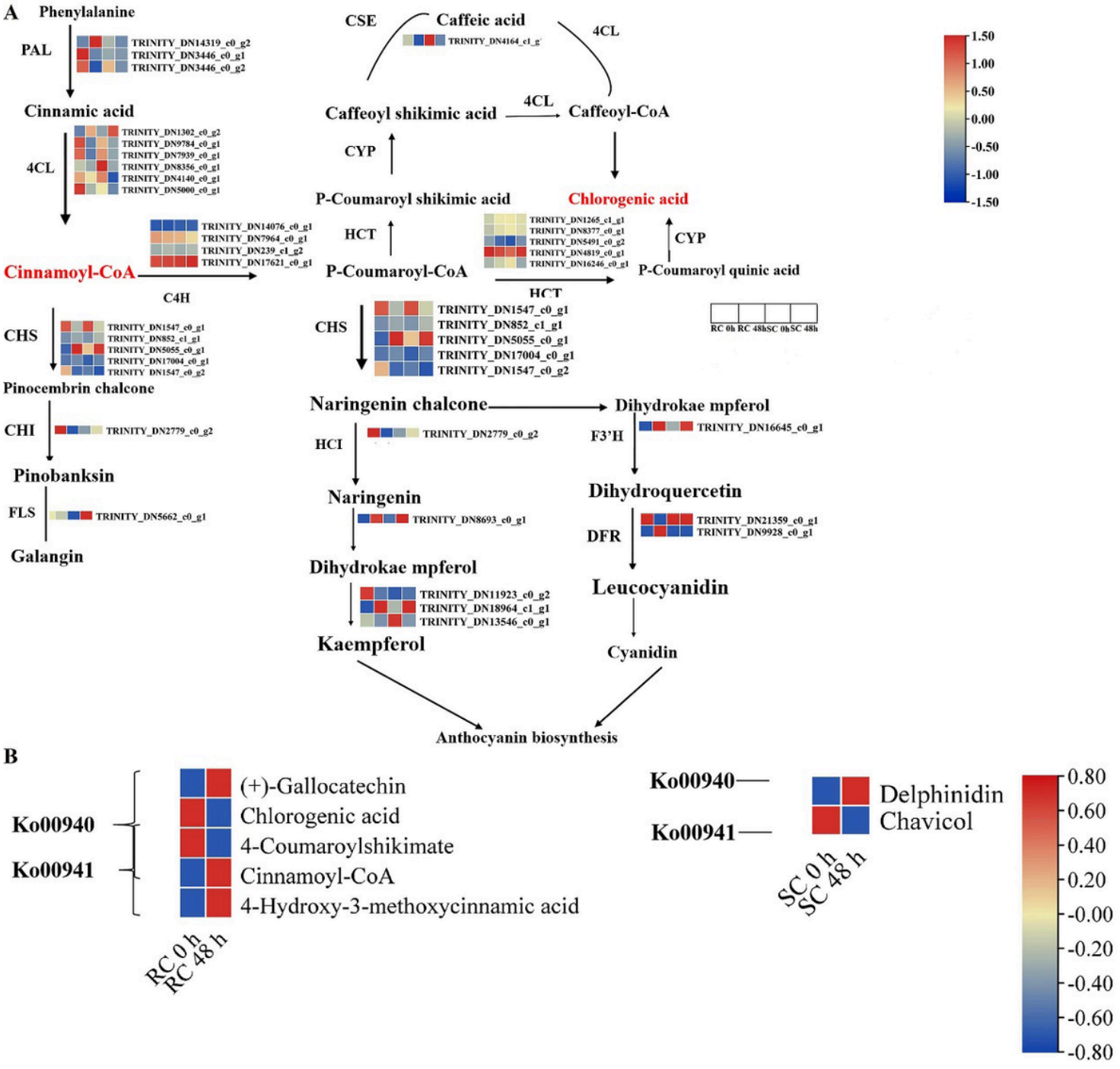

Figure 9

Transcriptional and metabolic analysis of important dam and DEGs related to the biosynthesis of anthocyanin under low-temperature stress. Colored boxes indicate the metabolites observed in this pathway. This pathway shows only the DEGs that have been correlated with the metabolites from the combined analysis of transcriptomes and metabolomes. (A) The map of integrative analysis in anthocyanin metabolites and their biosynthesis-related key enzymes. (B) Heatmap of DAMs enriched biosynthesis of the anthocyanin pathway. RC: cold-tolerant new line of P4; SC: cold-sensitive material of 13709.

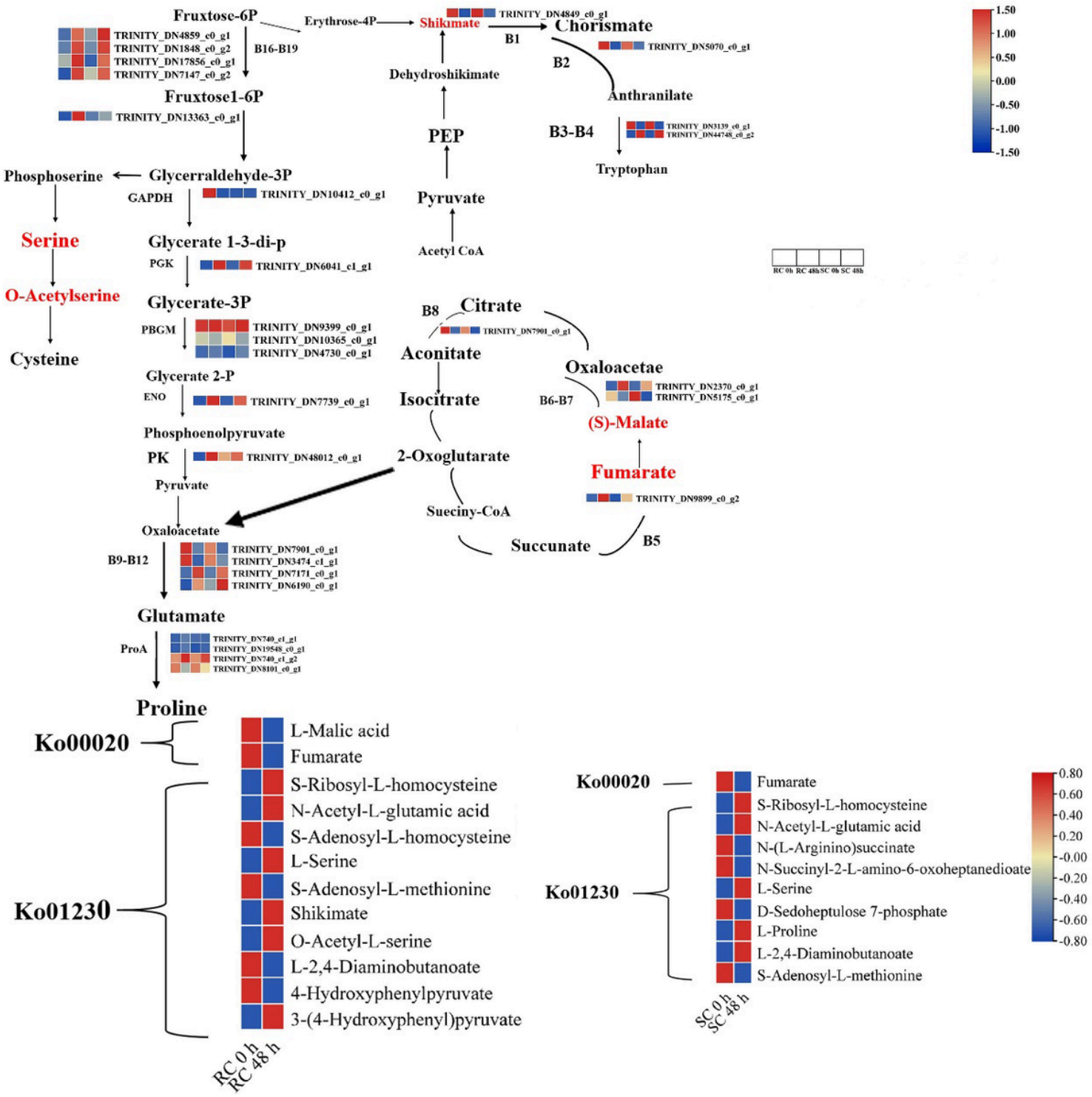

Figure 10

Screening for maps of metabolic pathways involving key differentially expressed metabolites. (A) The pathway map includes mainly biosynthesis of amino acids and tricarboxylic acid (TCA pathway). (B) Heatmap of DAMs enriched biosynthesis of amino acids and tricarboxylic acid (TCA pathway). RC: cold-tolerant new line of P4; SC: cold-sensitive material of 13709.

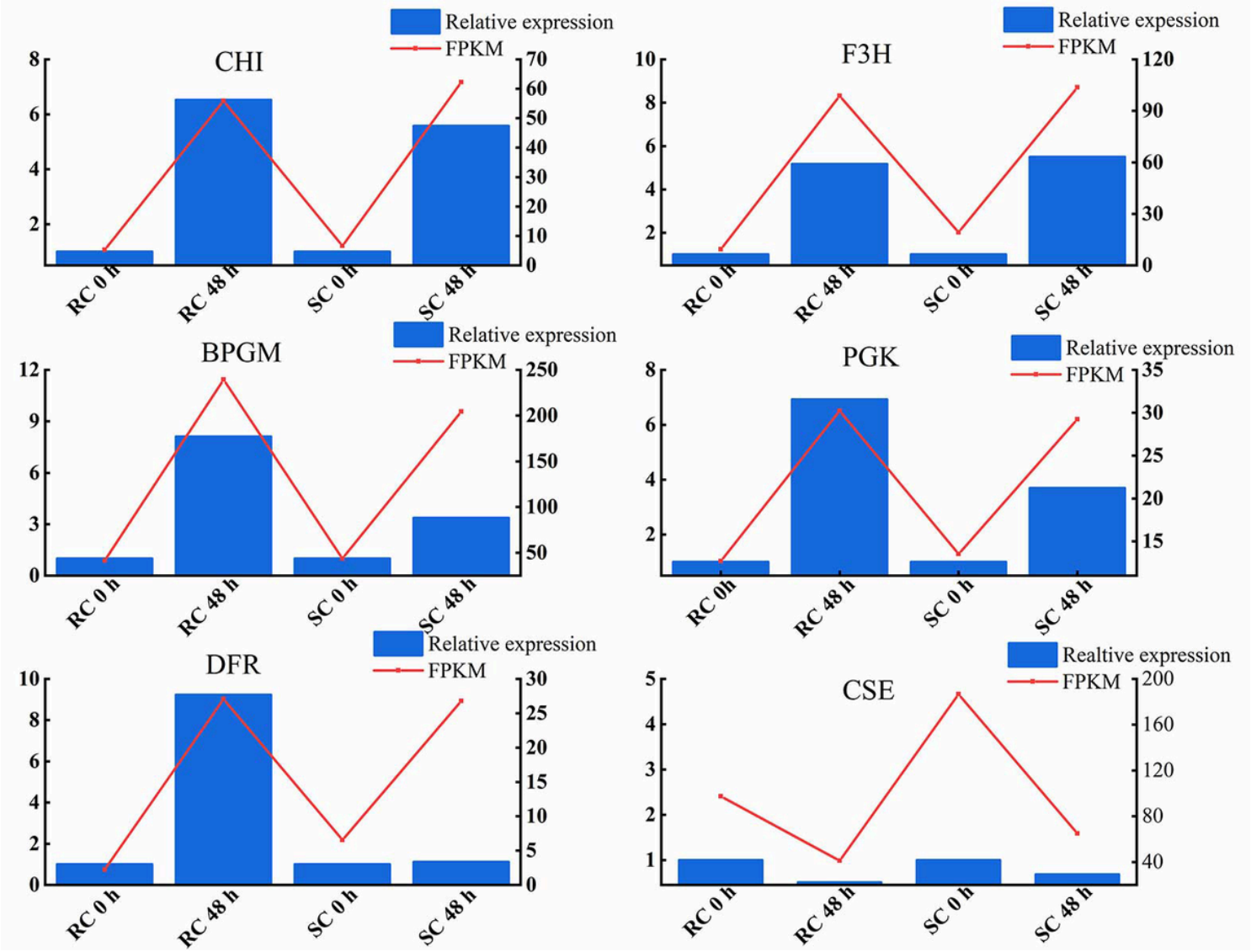

Figure 11

Expression profiles of six candidate genes by qRT-PCR and RNA-seq. The left and right ordinates represent the relative expression levels determined by qRT-PCR and RNA-seq, respectively. RC: cold-tolerant new line of P4; SC: cold-sensitive material of 13709.

Supplementary Files

This is a list of supplementary files associated with this preprint. Click to download.

- SupplementaryFiguresandTables.docx
- image1.png